JOURNAL OF MATERIALS SCIENCE 28 (1993) 4153–4158

Mechanical properties and failure of etched UHMW–PE fibres

M. S. SILVERSTEIN*, O. BREUER
Department of Materials Engineering, Technion-Israel Institute of Technology, Haifa 32000, Israel

The structural hierarchy of fibrillar ultra-high molecular weight polyethylene (UHMW–PE) fibres is investigated and related to fibre mechanical properties. Chemical etching has been used to change the surface properties of these UHMW–PE fibres through the removal of a skin layer and UHMW–PE oxidation. The physical and chemical changes to the fibre surface introduced by etching affect single-fibre mechanical properties. The effects of etchant and etching time on failure properties and mechanisms is discussed. The decrease in failure strain and strength with etching is associated with the change from an energy-absorbing fibril delamination failure to brittle fracture.

1. Introduction

1.1. Ultra-high molecular weight polyethylene fibres

Ultra-high molecular weight polyethylene (UHMW–PE) fibres are one of the more advanced polymer fibres in the high-performance fibre field [1]. A high degree of orientation in the fibres has been achieved through a gel-spinning process. Oriented microfibrils, blocks of densely packed crystalline areas connected by oriented amorphous tie molecules, tens of nanometres in diameter exist within the fibre [2, 3]. The ultra-high specific strength, ultra-high specific modulus, and extraordinary impact resistance are properties of interest for advanced aerospace, military, automotive, and biomedical applications. The greatest drawback to using these fibres in composite material applications has been their poor adhesion to polymer matrices.

1.2. Surface modification through etching

Several methods of fibre-surface treatment have been used in an attempt to improve the properties of UHMW–PE fibre-reinforced composite materials by enhancing adhesion [4]. Chemical, flame, corona, and plasma etching have been used to treat polyethylene surfaces [5]. Some treatments, notably plasma etching, have met with commercial success for these fibres.

Chemical etching is a popular method of surface modification that changes both surface chemistry and surface roughness. The modification mechanism consists of the abstraction of hydrogen atoms from the polymer backbone and their replacement with polar groups from the oxidizing etchants. Chromic acid [6] and potassium permanganate [7] have been used as etchants for polyethylene. Chromic acid, potassium permanganate and hydrogen peroxide are the oxidants studied in this research.

1.3. Effects of etching on composite properties

Composite properties are dependent on stress transfer through the fibre–matrix interface [8]. Enhanced interfacial adhesion improves stress transfer and is expected to improve composite properties. The single-fibre strength and failure strain, however, may be altered by the polymer degradation associated with adhesion-enhancing surface treatments. Chemical etching can embrittle the polymer and create flaws on the fibre surface. The etching process is expected to diminish fibre strength and failure strain. Surface treatments for composite applications must strike a balance between adhesion enhancement and single-fibre property degradation.

The structure and surface chemistry [9], wettability [10], and adhesion [11] of these chemically etched fibres has been studied. This paper will focus on the effects that chemical etching has on single-fibre mechanical properties. The relationships between these properties and changes on the fibre surface will be discussed.

2. Experimental procedure

2.1. Materials

The UHMW–PE ($M_w = 1.5 \times 10^6$) fibre was a 120 filament Spectra-1000 tow of 650 denier (g/9000 m) from Allied Fibre Inc., VA. The chromic acid etching solution was prepared by mixing potassium dichromate (IV) ($K_2Cr_2O_7$), sulphuric acid (H_2SO_4) and

* Author to whom all correspondence should be addressed.

0022–2461

distilled water in a 7:150:12 mass ratio. The potassium permanganate ($KMnO_4$) etching solution was prepared by mixing aqueous 0.2 M $KMnO_4$ with aqueous 0.2 M nitric acid (HNO_3) in a ratio of 4:1. The hydrogen peroxide (H_2O_2) etching solution was 30% H_2O_2 in an aqueous solution.

2.2. Chemical etching

The fibres were separated from the tow and left in an etching solution at room temperature. The etching times used were 5 min, 4 h and 24 h. After etching the fibres were first washed in running distilled water and then in ethanol. The fibres were dried in a vacuum oven at room temperature for 12 h. The fibre surfaces were gold coated for surface structure characterization in a Jeol-840 scanning electron microscope (SEM).

2.3. Mechanical properties

Single filaments separated from the tow were tested on an Instron tensile testing machine. A cross-sectional area of 620 μm^2 was used for the stress calculations based on an UHMW–PE density of 970 $kg\,m^{-3}$. The fibres were held in capstan tensile grips illustrated schematically in Fig. 1. The distance between the grips was taken as the apparent length. The contribution of the fibre ends to the true length was determined by the grip dimensions and by comparing the experimental results for various apparent initial lengths.

The tensile tests were conducted with an apparent initial length of 40 cm. The crosshead speed used was 20 cm min^{-1}, yielding an apparent strain rate of 50% min^{-1}. The properties cited are an average of 15–20 fibres. The modulus was calculated from the initial slope of the stress–strain curve. Gold-coated fracture surfaces were examined in the SEM.

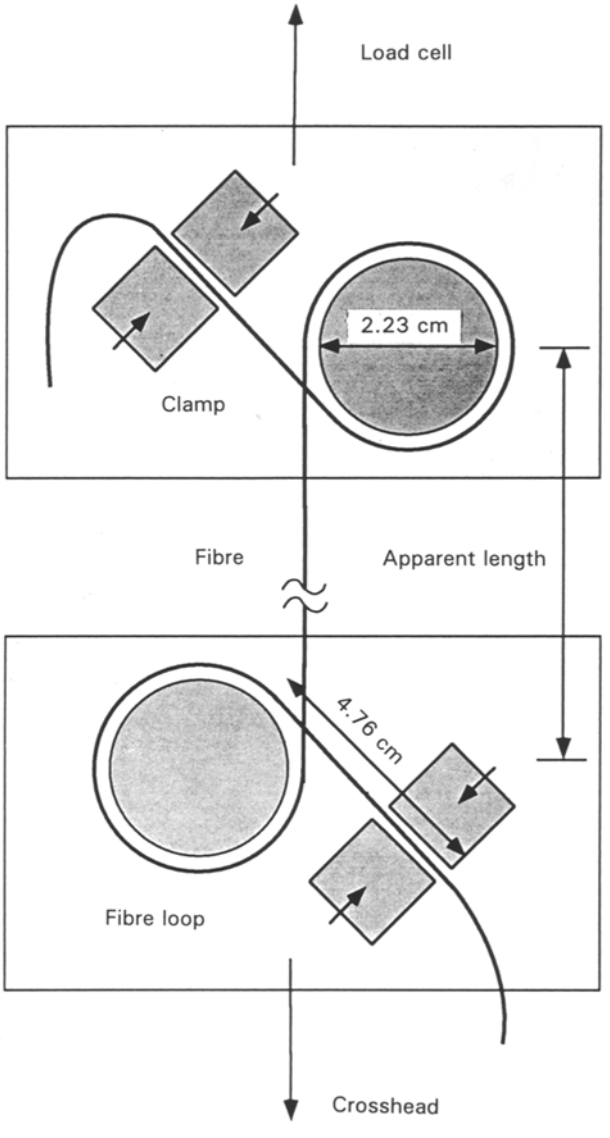

Figure 1 Schematic diagram of capstan fibre tensile grips.

3. Results and discussion

3.1. Surface structure

The changes in fibre-surface roughness are seen in the scanning electron micrographs in Fig. 2. The smooth surface in Fig. 2a is that of an as-received UHMW–PE fibre. The barely discernible ridges on the surface about 10 μm peak-to-peak, reflect the roughly circular but irregular fibre cross-section. The corrugated surfaces in Fig. 2b and c are seen after etching with chromic acid for 4 h at room temperature. There is no discernible change in fibre diameter or structure on further etching.

The etching process rapidly removes an outer "skin" layer revealing a fibrillar UHMW–PE fibre structure. The rapid etching of the skin indicates that it is not UHMW–PE which is relatively unaffected by etching. The skin is most likely formed of low molecular weight fragments and solvent excluded during the crystallization process. All the etchants remove enough skin to reveal a fibrillar structure. This structure is most clearly seen after chromic acid etching, indicating that chromic acid is the more powerful etchant.

UHMW–PE fibrils hundreds of nanometres in diameter are highly oriented along the fibre axis in Fig. 2b. Fibrils organized in 5 μm bundles yield the irregular 30 μm fibre cross-section. Microfibrillar ties tens of nanometres in diameter connect the fibrils in Fig. 2c. The fibrils themselves seem to be constructed of microfibrillar units corresponding to the organized structures formed by UHMW–PE crystalline blocks [3]. The UHMW–PE structural hierarchy is illustrated schematically in Fig. 3. The illustration depicts highly oriented microfibrils organized into larger fibrillar structures. Highly oriented and highly interconnected fibrils are organized in bundles within the fibre. A skin layer surrounds the highly oriented and organized fibrillar structure. This fibrillar structural hierarchy is similar to those seen for liquid crystalline polymers and biological systems such as tendon [12].

3.2. Tensile properties: as-received fibres

The failure strain, (ε_b), fibre strength, (σ_b), and modulus, E, are significant parameters in composite material design. The failure strain calculation depends on the correct determination of length. The apparent length, the distance between capstan grips, is less than

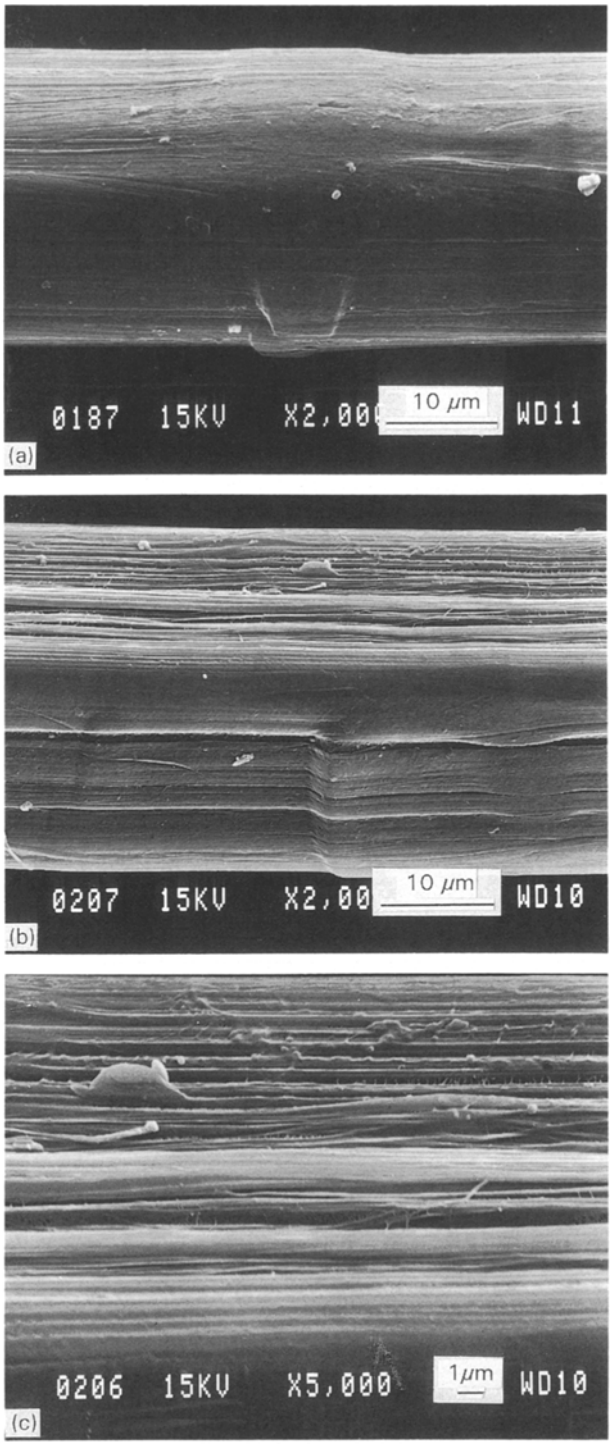

Figure 2 Scanning electron micrographs of fibres. (a) As-received; (b) after 4 h etch in chromic acid; (c) after 4 h etch in chromic acid.

the real length which includes the length of fibre ends wrapped around the grips. The length difference, L_e, between the real length and the apparent length can be determined from the grip geometry or from the interpretation of the data. An estimated $L_e = 21.3$ cm can be derived from the grip dimensions in Fig. 1. The apparent failure strain, ε_{ba}, based on the apparent length decreases with increasing apparent initial length, L_{0a}, in Fig. 4. The failure strain can be calculated from ε_{ba} using Equation 1 if L_{0a} is known and L_e is determined.

$$\varepsilon_b = \frac{\varepsilon_{ba}}{\left(1 + \frac{L_e}{L_{0a}}\right)} \quad (1)$$

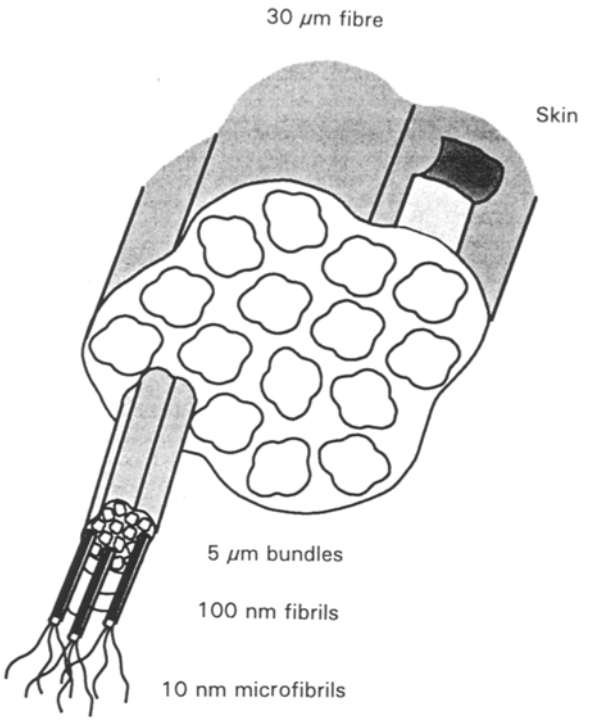

Figure 3 Schematic illustration of UHMW-PE fibre's fibrillar structural hierarchy.

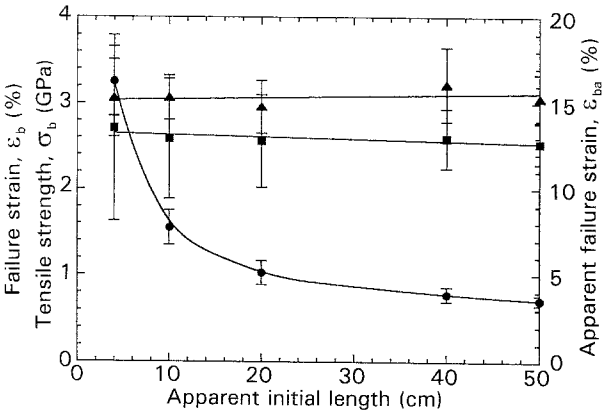

Figure 4 Tensile failure properties of as-received fibres as a function of initial fibre length. (●) ε_{ba}, (■) ε_b, (▲) σ_b.

L_e was chosen such that the deviation from the average ε_b for different L_{0a} was minimized. The best-fit value for L_e of 22 cm is close to that derived from the grip dimensions. Using Equation 1 yields an average failure strain of 2.5%, similar to the literature value of 2.7%. The 12% standard deviation in ε_b among the different L_{0a} is typical of fibre failure strains. The failure strain is independent of apparent initial length in Fig. 4. The fibre tensile strength is also independent of L_{0a} in Fig. 4, as expected. The strength of 3.2 GPa with a typical 13% standard deviation is close to the literature value of 3 GPa.

The tensile modulus, E, is, like elongation, dependent on the correct determination of length. The apparent modulus, E_a, based on the apparent length increases with increasing L_{0a} in Fig. 5. Here again there is a length difference, L'_e, between the real length and apparent length. L'_e, the length correction at small strains, may not be equal to L_e, the length correction

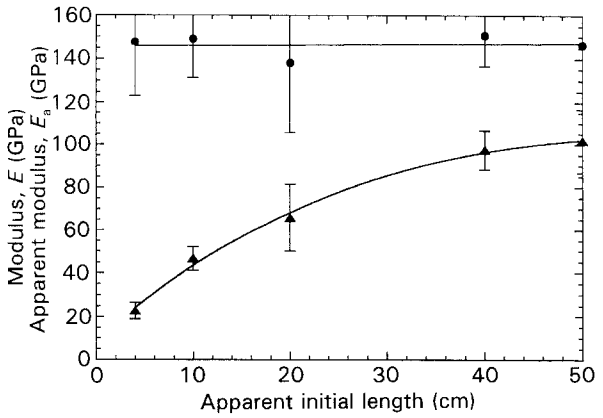

Figure 5 Tensile modulus of as-received fibres as a function of initial fibre length. (▲) E_a, (●) E.

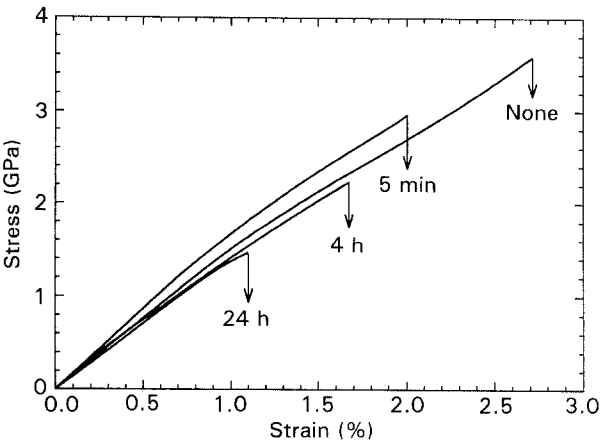

Figure 6 Typical stress–strain curves of fibres etched in chromic acid for various times.

at the failure strain. The modulus can be calculated from E_a using Equation 2 if L_{0a} is known and L'_e is determined

$$E = E_a\left(1 + \frac{L'_e}{L_{0a}}\right) \quad (2)$$

L'_e was chosen such that the deviation from the average E for different L_{0a} was minimized. The best-fit value for L'_e was also 22 cm, yielding an average modulus of 149 GPa. The 12% standard deviation in E among the different L_{0a} is typical of fibre moduli. The modulus is independent of apparent initial length in Fig. 5. The difference between the average modulus and the literature value of 172 GPa may be related to the experimental technique.

The identical length correction of 22 cm applies for both the initial and failure strains. This length correction and the estimated cross-sectional area were used to plot stress–strain curves from force–displacement data. The tensile tests were performed at the maximum achievable apparent initial length of 40 cm (a true initial length of 62 cm) in order to minimize the significance of the length corrections in Equations 1 and 2. The apparent strain rate of 50% min^{-1} is equivalent to a strain rate of 32% min^{-1}.

3.3. Tensile properties: etched fibres

The stress–strain curves of typical as-received and chromic acid etched fibres in Fig. 6 show significant changes in mechanical properties with etching time. The curves can be described as being formed of two linear portions, one with a larger slope at low strains and the other with a smaller slope at high strains. The tensile properties are listed in Table I for the various etchants and etching times.

The changes in tensile properties during chromic acid etching are illustrated more clearly in Fig. 7. The tensile modulus remains constant at about 150 GPa for up to 24 h etching. The failure strain undergoes an immediate step-like 20% reduction after 5 min etching and continues to decrease at a slower but constant rate with further etching. The failure strain is reduced to 45% of its original value after 24 h etching. The tensile strength exhibits the same behaviour as the failure strain. There is an immediate step-like 20% decreases in strength after 5 min etching. The strength continues to decrease at a slower but constant rate with further etching and is reduced to 50% of its original value after 24 h etching.

TABLE I Tensile properties of etched UHMW–PE fibres

Etch	Time	E(GPa)	σ_b(GPa)	ε_b(%)
None	–	149 ± 18	3.15 ± 0.40	2.52 ± 0.29
Chromic acid	5 min	150 ± 28	2.54 ± 0.41	1.98 ± 0.26
	4 h	155 ± 15	2.37 ± 0.38	1.57 ± 0.19
	24 h	145 ± 23	1.62 ± 0.37	1.18 ± 0.21
Potassium permanganate	5 min	152 ± 17	2.87 ± 0.34	2.35 ± 0.33
	4 h	155 ± 18	2.86 ± 0.29	2.19 ± 0.27
	24 h	153 ± 21	1.77 ± 0.38	1.96 ± 0.21
Hydrogen peroxide	4 h	146 ± 22	2.37 ± 0.35	2.38 ± 0.36

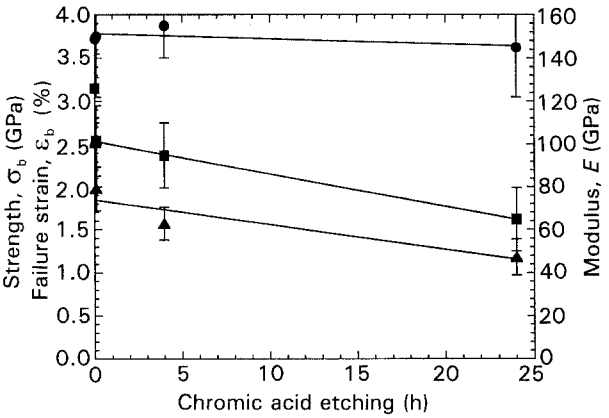

Figure 7 Mechanical properties of fibres etched in chromic acid as a function of etching time. (●) E, (■) σ_b, (▲) ε_b.

The tensile properties of the potassium permanganate and hydrogen peroxide etched fibres exhibit the same type of trends as the chromic acid etched fibres. The modulus is relatively constant while both the tensile strength and failure strain decrease with time. The variation in tensile properties with etching time for potassium permanganate etched fibres is seen in Fig. 8. There is an immediate step-like decrease of 10% in strength and failure strain after 5 min etching.

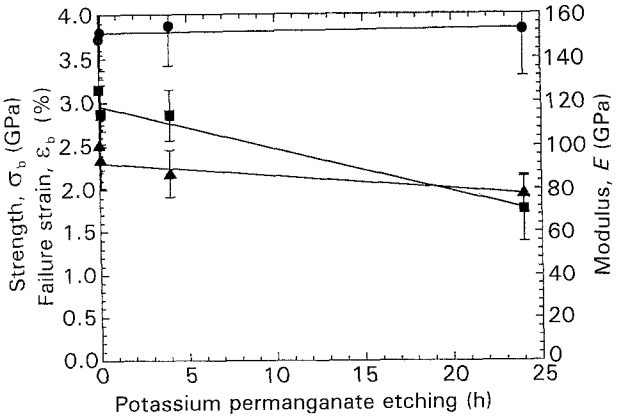

Figure 8 Mechanical properties of fibres etched in potassium permanganate as a function of etching time. (●) E, (■) σ_b, (▲) ε_b.

The strength and failure strain diminish at a slower but more constant rate with continued etching. The strength and failure strain are reduced to 55% and 75% of their original values, respectively, after 24 h etching. Both the immediate and the overall decrease in tensile properties is most significant in the chromic acid etched fibres, again indicating that chromic acid is the more powerful etchant.

3.4. Failure mechanism

The failure mechanism of the fibres plays an integral role in determining their mechanical properties. The as-received fibres fail through the fibril delamination seen in Fig. 9a. This failure takes place at different levels of the fibrillar structural hierarchy depicted in Fig. 3. The submicrometre fibrils, seen on the fibre surface in Fig. 2b, fail and delaminate from the fibre structure resulting in a "split ends" appearance.

The fibres etched 24 h in chromic acid fail in a brittle manner. The failure surface in Fig. 9b is perpendicular to the direction of applied force, typical of brittle fractures. The decrease in strength, failure strain, and work to failure (area under the stress–strain curves in Fig. 6) with etching time corresponds with this change from fibril delamination to brittle fracture. The work to failure is reduced by 40% after 5 min etching in chromic acid and is reduced to 20% of its original value after 24 h. This great reduction in work to failure reflects both the decrease in failure strength and strain. The reduction in all three failure properties (normalized by the as-received fibre properties) with chromic acid etching time is seen in Fig. 10.

The fibril delamination failure mechanism enhances toughness. The fibrillar hierarchy distributes the load efficiently in an energy-absorbing manner throughout various structural levels. The fibrillar structures in liquid crystal polymer blend fibres were similarly associated with the ultimate properties for various blend compositions [13]. These significant changes in single-fibre mechanical properties and failure mechanisms will be reflected in composite material properties. Composite design must take both the enhanced adhesion [11] and the degraded mechanical properties into account.

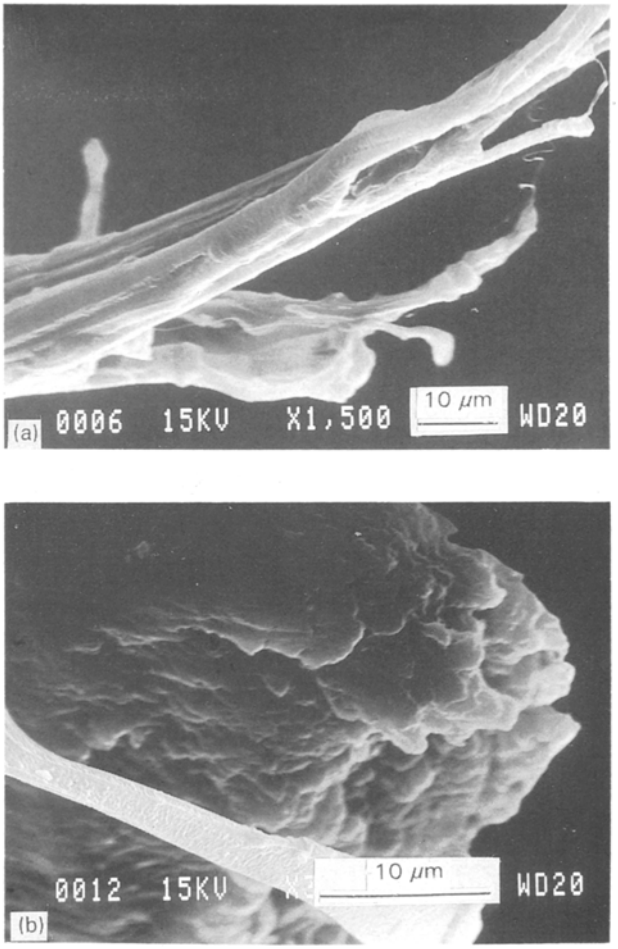

Figure 9 Scanning electron micrographs of fibre fracture surfaces. (a) As-received; (b) after 24 h etch in chromic acid.

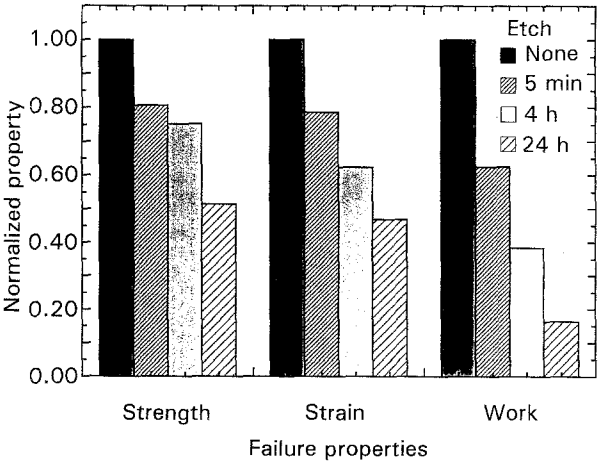

Figure 10 Reduction in strength, failure strain, and work to failure with time for fibres etched in chromic acid. The properties are normalized by the as-received fibre properties.

5. Conclusions

The UHMW–PE fibres possess a fibrillar structural hierarchy. Highly oriented fibrils (≈ 100 nm) are formed from and are interconnected by microfibrils (≈ 10 nm). Bundles of fibrils covered by a non-UHMW–PE skin form the irregularly shaped fibres (≈ 30 μm). The skin is rapidly removed by etching and the fibrillar structure revealed. Chromic acid is a

powerful etchant and reveals the fibrillar structure clearly.

The etching produces an immediate step-like decrease in failure strength and strain. The failure strength and strain continue to decrease at a slower but constant rate with further etching. Chromic acid etching produces an immediate 20% reduction in failure properties which reach 50% of their original value after 24 h etching. The significant decrease in toughness with etching is related to the change in failure mechanism from energy-absorbing fibril delamination to brittle fracture. The structural and chemical changes to the fibre surface associated with etching embrittle the fibre and reduce its load-bearing capability.

References

1. S. BORMAN, *Chem. Eng. News* 9 *October* (1989) 23.
2. P. J. BARHAM and A. KELLER, *J. Mater. Sci.* **20** (1985) 2281.
3. D. C. PREVORSEK, H. B. CHIN, Y. D. KWON and J. E. FIELD, *J. Appl. Polym. Sci. Appl. Polym. Symp.* **47** (1991) 45.
4. B. TISSINGTON, G. POLLARD and I. M. WARD, *J. Mater. Sci.* **26** (1991) 82.
5. A. J. KINLOCH, "Adhesion and Adhesives" (Chapman and Hall, New York, 1987) p. 112.
6. D. BRIGGS, D. M. BREWIS and M. B. KONIECZO, *J. Mater. Sci.* **11** (1976) 1270.
7. R. H. OLLEY, A. M. HODGE and D. C. BASSET, *J. Polym. Sci. Polym. Phys. Ed.* **17** (1979) 627.
8. L. E. NIELSEN, "Mechanical Properties of Polymers and Composites", Vol. 2 (Marcel Dekker, New York, 1974) p. 471.
9. M. S. SILVERSTEIN, O. BREUER and H. DODIUK, in preparation.
10. M. S. SILVERSTEIN and O. BREUER, *Polymer*, accepted.
11. *Idem., J. Mater. Sci.* accepted.
12. E. BAER, *Sci. Am.* **255** (1986) 156.
13. J. X. LI, M. S. SILVERSTEIN, A. HILTNER and E. BAER, *J. Appl. Polym. Sci.* **44** (1992) 1531.

Received 10 June 1992
and accepted 3 February 1993